

16 **ABSTRACT**

17 Wastewater-based surveillance systems can track trends in multiple pathogens simultaneously by
18 leveraging efficient, streamlined laboratory processing. In Switzerland, wastewater surveillance is
19 conducted for fourteen locations representing 2.3 million people, or 26% of the national population, with
20 simultaneous surveillance of four respiratory pathogens. Trends in respiratory diseases are tracked
21 using a novel, six-plex digital PCR assay targeting Influenza A, Influenza B, Respiratory Syncytial Virus,
22 and SARS-CoV-2 N1 and N2 genes, as well as Murine Hepatitis Virus for recovery efficiency control.
23 The multiplex assay was developed to ensure sensitivity and accurate quantification for all targets
24 simultaneously. Wastewater data is also integrated with disease data obtained through both a
25 mandatory disease reporting system and the Swiss Sentinel System (Sentinella), a voluntary reporting
26 system for general practitioners. Comparisons between wastewater data and case data from July 2023
27 through July 2024 demonstrate a high level of agreement, specifically for Influenza A, SARS-CoV-2,
28 and Respiratory Syncytial Virus. Lower correspondence is observed for Influenza B, which highlights
29 challenges in tracking disease dynamics during seasons without pronounced outbreak periods.
30 Wastewater monitoring further revealed that targeting the N1 or N2 gene led to divergent estimates of
31 SARS-Cov-2 viral loads, highlighting the impact of mutations in the target region of the assay on tracking
32 trends. The study emphasizes the importance of an integrated wastewater monitoring program as a
33 complementary tool for public health surveillance by demonstrating clear concordance with clinical data
34 for respiratory pathogens beyond SARS-CoV-2.

35 INTRODUCTION

36 Respiratory infections are a leading cause of morbidity and mortality worldwide – particularly in children
37 and the elderly¹. Such infections are commonly caused by viral pathogens, including Influenza A (IAV)
38 and B (IBV), Respiratory Syncytial Virus (RSV), and SARS-CoV-2. Infections from respiratory viruses
39 typically follow a seasonal pattern, with one or two peaks annually, though in many countries influenza
40 transmission is identified year-round². Our knowledge about respiratory virus epidemiology and infection
41 dynamics is overwhelmingly driven by clinical data reporting systems. However, such systems can be
42 subject to bias, likely underestimating the disease prevalence³, or incompletely capturing dynamics due
43 to changes in testing or reporting strategies or changes in population behavior seeking medical care.

44 Wastewater-based surveillance (WBS) is proposed as an alternative and/or complementary option for
45 tracking respiratory viruses^{4,5}. WBS relies on wastewater analysis for detecting genetic material of a
46 target pathogen, often by implementing molecular-based assays, such as quantitative PCR (qPCR) and
47 digital PCR (dPCR). The COVID-19 pandemic has highlighted the potential and advantages of WBS^{6,7},
48 which is now applied worldwide.

49 WBS allows a broad, population-level perspective by sampling wastewater, offering insights into the
50 trends of entire communities or regions from just one 24-hour composite wastewater sample per day.
51 Further, WBS is useful as a complementary tool to traditional surveillance methods, providing data that
52 can enhance the accuracy and timeliness of public health interventions⁸⁻¹⁰. Indeed, previous studies
53 reported a strong association between wastewater viral concentrations and reported clinical cases,
54 suggesting that when both surveillance strategies are sensitive enough, the resulting data solidly
55 correspond.

56 WBS has been applied to the detection of diverse respiratory pathogens beyond SARS-CoV-2, including
57 RSV and influenza viruses¹¹⁻¹³. Tracking pathogen concentrations in settled solids and wastewater
58 influent aligns with available clinical data, which often relies on metrics such as clinical positive rates (as
59 in Hughes et al. for RSV) or influenza-like illnesses (as in Wolfe et al. and Zheng et al. for Influenza A).
60 Moreover, simultaneous detection of multiple pathogens in wastewater offers an efficient means of
61 monitoring distinct diseases. To achieve this multiplexing of pathogens, dPCR, compared to qPCR,
62 offers substantial potential¹⁴.

63 The wastewater monitoring program in Switzerland was initiated in July 2020 for the surveillance of
64 SARS-CoV-2, and subsequently expanded for the detection of IAV, IBV, and RSV, with the
65 implementation of a second multiplex dPCR assay¹⁵ in November 2022. To improve the workflow and
66 reduce costs of the surveillance program, we developed a novel multiplex dPCR assay for detecting
67 simultaneously the four target respiratory viral pathogens (IAV, IBV, RSV, and SARS-CoV-2) as well as
68 an additional quality control to measure recovery efficiency (Murine Hepatitis Virus, MHV). Here, we
69 report the development and application of the multiplex dPCR assay to the established wastewater
70 surveillance framework for monitoring in Switzerland.

71 RESULTS

72 Performance of the six-plex dPCR assay and quality control indicators

73 The six-plex dPCR assay, referred to as RESPV6, was designed for detecting six target genes with
74 specific fluorophores: SARS-CoV-2 N1 gene (SARS-N1, ATTO425), SARS-CoV-2 N2 gene (SARS-N2,
75 FAM), RSV N gene (RSV-N, ROX), IAV M gene (IAV-M, Cy5), IBV M gene (IBV-M, HEX), and MHV M
76 gene (MHV-M, Cy5.5). All selected targets produced clusters which were separable, allowing for
77 discrimination between positive and negative partitions, and between distinct targets (**Fig. 1**).

78 The assay was applied for monitoring wastewater between July 2023 and July 2024, leading to a total
79 of 13'028 individual dPCR reactions. Of those reactions, 7'795 were performed on wastewater samples
80 collected from 14 WWTPs (**Supplemental Table 1**), 2'482 were run for control purposes, and 2'751 for
81 assessing PCR inhibition. Altogether, we analyzed 3'538 distinct wastewater samples.

82 Since wastewater is a complex matrix and can contain inhibitors we determined the levels of PCR
83 inhibition present in the analyzed wastewater nucleic acid extracts, and repeated samples showing more
84 than 40% inhibition. For reactions that passed quality control (7'052/7'795), we observed a median PCR
85 inhibition of 3% (interquartile range [IQR] 14%). We observed a significant variation across different
86 locations (Kruskal-Wallis test, $p < 0.001$). The Dunn's multiple comparisons test displayed that samples
87 from Basel had a significantly higher level of inhibition (median of 7%) than other WWTPs, whereas
88 samples from Solothurn had lower level of inhibition compared to other WWTPs (median of -1%)
89 (**Supplemental Table S2**).

90 During this study, we observed dPCR reaction failure in a total of 743 reactions out of 7'795 (10%). Of
91 these, 121 failed because of high levels of inhibition (>40% inhibition, 16%), 303 due to a failed no
92 template control suggesting possible contamination of the sample (NTC, 40%), and 334 for insufficient
93 number of partitions (i.e., <15'000 droplets, 44%). Reaction failure resulted in data for 281 samples (8%)
94 being taken from a single replicate rather than the average of duplicates.

95 Based on the recovery of MHV, the recovery efficiency control, we observed a median recovery rate of
96 18% (IQR 38%) and an average of 30% ($\pm 27\%$), which was derived from running efficiency control in
97 3'951 dPCR reactions. We detected a significant difference among locations (Kruskal-Wallis test, $p <$
98 0.001). The Dunn's multiple comparisons test showed that samples from Basel had a significantly lower
99 extraction efficiency than other WWTPs (**Supplemental Table S3**).

100 Among the reactions containing wastewater extracts that passed quality control, we observed a median
101 number of partitions of 22'104 (IQR 4'726). Moreover, we estimated the volume of reaction mixture that
102 did not form partitions (dead volume) which showed that the median percentage of dead volume for
103 each reaction was 54% (IQR 10%).

104 Detection of viral pathogens in Swiss wastewater

105 Our dPCR analysis of 3'538 samples revealed that IAV was detected in 27% of the samples ($n = 941$),
106 IBV in 42% ($n = 1'491$), and RSV in 38% of the samples ($n = 1'338$). SARS-CoV-2 was detected in 99%
107 and 98% of the samples for the N1 and N2 genes respectively ($n = 3'499$, $n = 3'472$). Despite N1 and
108 N2 displaying a marked positive linear relationship ($R^2 = 0.97$), N2 values were generally higher than
109 N1 values (**Fig. 2**). Indeed, the ratio of N1 to N2 was 0.87 ± 0.33 (mean \pm standard deviation [s.d.]) ($n =$

110 3'538). Interestingly, we noted a shift in the ratio of N1 to N2 over the monitoring period. From July 2023
111 to January 2024 the ratio was constantly below one at all locations (0.71 ± 0.23 , $n = 1'648$), but then
112 returned to one after January 2024 (1.01 ± 0.35 , $n = 1'890$) ([Supplemental Fig. S1](#)).

113 **Viral loads of respiratory pathogens in Swiss wastewater**

114 We explored the epidemiology of the target respiratory viruses by observing the viral loads in
115 wastewater, expressed in gene copies per person per day ($\text{gc person}^{-1} \text{ day}^{-1}$), over time. To better
116 identify and interpret the trends, we calculated the median value over a centrally aligned seven-day
117 rolling period. This helped smooth fluctuations and outliers.

118 This observational period was strongly characterized by a considerable wave of SARS-CoV-2 loads,
119 detected in all 14 catchments, from October 2023 until February 2024 (**Fig. 3**). Each location was
120 characterized by an outbreak peak (i.e., maximum median value) between 9th November 2023 and 21st
121 December 2023. Lucerne displayed the highest load of $9.7 \times 10^8 \text{ gc person}^{-1} \text{ day}^{-1}$ on the 8th of
122 December 2023 (**Fig. 3C**). Importantly, a second peak of SARS-CoV-2 was identified in all catchments
123 starting in April 2024, particularly in Lausanne, where a clear second wave was visible and comparable
124 to the previous one (**Fig. 3N**).

125 The surveillance period was also characterized by the presence of the other measured pathogens IAV,
126 IBV, and RSV, though the concentrations and loads in wastewater were considerably lower than those
127 of SARS-CoV-2, differing by more than one order of magnitude (**Fig. 3**, **Fig. 4**). Between December
128 2023 and mid-March 2024, we encountered a seasonal outbreak of IAV. Maximum peaks were seen
129 within a one-month period (18th Jan – 16th Feb 2024) for 13 locations. The exception was Lugano where
130 the peak occurred earlier ([Supplemental Fig. S2A](#)). Moreover, Lugano had the highest peak value for
131 IAV among all locations, with $5.1 \times 10^7 \text{ gc person}^{-1} \text{ day}^{-1}$ on the 28th of December 2023 (**Fig. 4J**).
132 Between November 2023 and May 2024, we observed a wave of RSV, and peak values were identified
133 between 3rd December 2023 and 15th February 2024 for 13 locations, except for Solothurn which was
134 characterized by a peak in July 2023 (**Fig. 4I** and [Fig. S2C](#)).

135 Unlike SARS-CoV-2, IAV, and RSV outbreaks, which showed similar and comparable trends across
136 different Swiss locations, the trends for IBV were less clear, with fewer comparable and distinguishable
137 patterns among catchments ([Supplemental Fig. S2B](#)). As such we observe the peak values for IBV
138 over more than eight months (13th Nov 2023 – 12th Jul 2024).

139 **Comparison of viral loads in wastewater with clinical data from different sources**

140 At the national level, we observed consistent relationships between weekly wastewater viral loads and
141 weekly clinical cases from the Sentinella system for all four pathogens tracked (**Fig. 5**). We observed a
142 strong positive correlation between IAV RNA loads in wastewater and IAV clinical cases (Pearson
143 correlation, $r = 0.95$ [$p < 0.0001$]), between SARS-CoV-2 RNA loads and clinical cases ($r = 0.87$ [$p <$
144 0.0001]), and between RSV RNA loads and clinical cases ($r = 0.68$ [$p < 0.0001$]). The same analysis for
145 IBV showed a rather low correlation ($r = 0.28$ [$p = 0.04$]) (**Fig. 5B**).

146 Subsequently, we performed the same correlation coefficient analysis using clinical data publicly
147 available from the mandatory reporting system, which reports clinical positive cases per week for IAV,
148 IBV, and SARS-CoV-2. As expected, we observed higher correlation coefficients ($r = 0.99$ for IAV [$p <$

149 0.0001], $r = 0.44$ for IBV [$p = 0.0008$], and $r = 0.93$ for SARS-CoV-2 [$p < 0.0001$]), likely due to the better
150 spatial resolution of such data which is less prone to bias ([Supplemental Fig. S3](#)). Additionally, we
151 investigated the relationship between clinical data from Sentinella and from the mandatory reporting
152 system, and we observed very strong Pearson correlation coefficients for SARS-CoV-2 and IAV ($r =$
153 0.92 [$p < 0.0001$] and $r = 0.95$ [$p < 0.0001$]). However, the correlation for IBV was only moderate ($r =$
154 0.63 [$p < 0.0001$]).

155 From the mandatory reporting system, SARS-CoV-2 clinical data is also stratified geographically at the
156 cantonal level. Therefore, we investigated the relationships between viral RNA loads from each location
157 and the cases reported in the corresponding canton by computing Pearson correlation coefficients. We
158 observed strong correlations with coefficients ranging from 0.55 to 0.93 ([Supplemental Table S4](#)).

159 **Lag times between clinical cases and viral RNA loads in wastewater**

160 We used time-lagged cross-correlation to estimate lag times between wastewater viral loads and clinical
161 cases for all four pathogens. Our analysis of weekly data showed that for RSV, the maximum value was
162 reached at one week of lag, with wastewater data preceding clinical data ([Supplemental Fig. S5](#)).
163 However, the computed coefficient was only slightly higher compared to the value obtained without lag
164 (0.70 and 0.68 , respectively) ([Supplemental Table S5](#)). In contrast, for IAV, IBV, and SARS-CoV-2, the
165 highest Pearson correlation coefficient was identified with no lag.

166 To investigate if there was a lag within the first week, we used the clinical data obtained from the Swiss
167 Federal Office of Public Health (FOPH) with daily resolution, which was provided for SARS-CoV-2, IAV,
168 and IBV at the cantonal level. Therefore, we examined the correlations between viral RNA loads from
169 each catchment and the reported cases in the corresponding canton. Our analysis did not reveal a
170 consistent pattern of wastewater data preceding clinical data across all locations. Indeed, lag times for
171 SARS-CoV-2 ranged from 0-5 days, for IAV from 0-7 days, and for IBV from 1-14 days, wastewater
172 always being earlier.

173 Notably, we also observed lower correlation coefficients for SARS-CoV-2, when considering cantonal
174 data with daily resolution instead of weekly aggregation. Coefficients ranged from 0.22-0.81 compared
175 to 0.55-0.92. Moreover, as the 2023/2024 season was characterized by two waves of SARS-CoV-2, we
176 also computed correlation coefficients for each wave separately, and we observed that in the second
177 surge, values were generally ~2.5 times lower, with coefficients ranging from 0.09-0.56.

178 DISCUSSION

179 In this study, we report the successful development of a multiplex digital PCR (dPCR) assay targeting
180 four common respiratory viruses – Influenza A (IAV) and B (IBV), Respiratory Syncytial Virus (RSV),
181 SARS-CoV-2 (N1 and N2 genes) – and the internal control Murine Hepatitis Virus (MHV), an RNA virus
182 used to monitor recovery efficiency. The six-plex dPCR assay enables absolute target quantification
183 without the need for a standard curve for six targets simultaneously. A higher order of multiplexing can
184 be achieved through additional channels or by amplitude-based multiplexing¹⁴, broadening the panel of
185 detectable targets. Although we designed this assay for a 6-color system, it can be readily adapted to
186 meet other requirements, by modifying fluorophores or changing channels. We applied our assay to
187 Swiss wastewater samples within the scope of a previously established, national wastewater
188 surveillance program¹⁶. We obtained four or five samples per week from 14 different wastewater
189 treatment plants located across Switzerland, which collect the influent from more than one fourth of the
190 Swiss residential population. Detecting viral RNA in wastewater is challenging due to low concentrations
191 and the complexity of the matrix; indicating that efficient viral concentration methods are needed¹⁷. Here,
192 we used MHV as internal control for extraction efficiency, and observed a mean recovery of 30%, which
193 was close to the lower end of the range 26.7-65.7% found in a previous study that compared different
194 concentration methods¹⁸. Notably, the extraction method used in our study which relies on direct
195 capture, was not evaluated in the study. The reduced recovery could have been influenced by the
196 contained wastewater volume employed (40 ml). Future efforts should focus on increasing sensitivity,
197 by for example, increasing the volume of samples processed or improving recovery efficiency.

198 We detected and measured RNA from all assessed respiratory viruses, suggesting that our six-plex
199 dPCR assay was specific to the selected genomic regions, and that our procedures were sufficiently
200 sensitive to capture the clinically observed outbreaks for IAV, RSV, and SARS-CoV-2. The dPCR assay
201 targeted both the SARS-CoV-2 N1 and N2 genes. Indeed, the use of various viral targets is generally
202 advised, as the selection of only one could increase the rate of false-negatives¹⁹. However, this is not
203 always feasible in practice, as it would greatly increase the required degree of multiplexing. Here, N1
204 and N2 markers showed strong agreement, despite N2 concentrations typically being higher than those
205 of N1. Specifically, the N1 to N2 ratio was constantly below one until around January 2024, before
206 returning to one. This observed discrepancy may have been triggered by mutations in the N1 probe
207 binding region, which could reduce affinity, as proposed and demonstrated by Sun and colleagues²⁰.
208 However, we identified a point mutation (T28297C), positioned in the N1 forward primer binding site,
209 which was present in 47.7% of the sequenced strains over the study period²¹. From July 2023 to January
210 2024, the percentage of strains carrying the mutation was 57.8%, which decreased to 4.3% from
211 January to July 2024, corresponding to the timing of the N1/N2 ratio shift towards one. This observation
212 suggests that T28297C lead to the decrease in N1/N2 ratio, highlighting how measured viral loads are
213 impacted by the mutation landscape. By having multiple targets for a pathogen, decreasing primer/probe
214 efficiency due to mutation can be more readily identified and primers or probes can be redesigned as
215 required to ensure continuing assay performance.

216 We report that the 2023/2024 winter season in Switzerland was characterized by a substantial outbreak
217 of SARS-CoV-2, with peak loads 10 to 100 times higher than those of other investigated respiratory

218 viruses. This observed trend is consistent with previously reported loads^{15,22}. The divergence in
219 magnitude is potentially attributed to the higher transmissibility rate of SARS-CoV-2 compared to that of
220 influenza and other seasonal respiratory viruses²³. Notably, it could also be due to higher concentrations
221 of SARS-CoV-2 RNA in feces of infected people relative to IAV, IBV, and RSV. Importantly, this winter
222 season was dominated by the JN.1 variant²¹, which appears to be more transmissible than its parental
223 virus^{24,25}. In some catchments, we identified a second wave of SARS-CoV-2, which was smaller and
224 driven by the KP.2 variant²⁶.

225 Focusing on flu-season, IAV evidently prevailed over IBV, which was less abundant in wastewater and
226 less reported in clinical settings. Despite the low number of positive cases of IBV, we detected its RNA
227 in wastewater in 30% of the wastewater samples, which was not achievable by other studies^{27,28}.
228 Measurements of RSV in wastewater indicated the presence of a clear outbreak, which occurred
229 between November 2023 and May 2024. Wastewater surveillance of RSV nicely demonstrates how
230 wastewater data is valuable to get an insight into the epidemiological situation, in absence of a complete
231 reporting system, as RSV infections are not subjected to mandatory declaration requirements in
232 Switzerland.

233 For all viruses we observed occasional high measurement values. It is known that there are several
234 sources of uncertainty in wastewater-based surveillance (WBS)²⁹, and, despite attempts to control for
235 some (e.g. inhibition), there are several which cannot be controlled for and their impact on concentration
236 measurements remains to be elucidated. We therefore use a seven-day rolling median to determine a
237 smoothed trend. Further work to understand specificities of wastewater viral concentration data could
238 provide better methods for determining the average of technical replicates, generating a smooth signal
239 or identifying outlier data points.

240 WBS has been extensively proposed as a useful tool for complementing clinical data, leading to a better
241 understanding of respiratory diseases and identifying potential trends. In this study, we identified very
242 strong correlations between wastewater viral loads and clinical cases, particularly for SARS-CoV-2 and
243 IAV, as their occurrence was high during the monitoring period, and for RSV. The only exception was
244 IBV, where we did not identify a strong correlation. In this case, wastewater data did not show a seasonal
245 outbreak, whereas clinical cases collected through the mandatory reporting system indicated an
246 outbreak (**Supplemental Fig. S3C**). Notably, cases from Sentinella and from the mandatory reporting
247 system agreed only moderately. This might indicate that IBV was not causing a highly symptomatic
248 infection or potentially had lower levels of viral shedding. Interestingly both the mandatory reporting and
249 Sentinella systems indicate a roughly 80:20 ratio of IAV to IBV cases. The ability of the mandatory
250 reporting system to capture the IBV outbreak is likely due to the greater number of cases reported in
251 this way (n = 120'862 compared to n = 2'316).

252 Previous studies focusing on SARS-CoV-2 showed that the number of clinical cases follows viral titers
253 in wastewater by variable lag times³⁰⁻³³. Our time-lagged cross-correlation analysis on four pathogens
254 indicates that wastewater might serve as a leading indicator. However, we did not observe a uniform
255 pattern of wastewater data consistently preceding clinical data across all sites, suggesting that some
256 location-specific effects might exist. Differences might arise based on how representative the cantonal

257 clinical data is when compared to the localized catchment viral load measurements. Moreover, several
258 factors should be considered, such as population effects, including the proportion of vaccinated
259 individuals and mobility behavior; and sewer network characteristics, like the influence of industrial
260 discharge, and rainfall events²⁹. Indeed, industrial wastewater might contain chemicals that could
261 degrade RNA molecules; and rainfall events can introduce a dilution effect, leading to lower measured
262 levels, which might fall below the limit of detection.

263 In the context of SARS-CoV-2, when comparing the relationship between wastewater loads and case
264 data, we noticed that correlation coefficients were higher when clinical data were aggregated on a
265 weekly level compared to daily data. This observation might be attributable to the intra-week variability
266 in case reporting, or to a reduction of daily fluctuations of wastewater measurements when averaging
267 over seven days. Additionally, as the monitoring period was characterized by two distinct waves, we
268 observed a weaker relationship between wastewater loads and clinical cases during the spring-summer
269 surge. This observation could be attributable to a decline in testing behavior during summer months or
270 to the KP.2 variant potentially causing a less symptomatic infection.

271 Our study possesses some limitations. Despite reporting good assay sensitivity, considerable variations
272 in pathogen concentrations in wastewater might lead to a reduction in sensitivity for detecting low-
273 prevalence targets. Our results strongly suggest that WBS can be particularly valuable in settings where
274 traditional surveillance systems are limited or inaccessible, such as resource-constrained areas or
275 regions with inadequate healthcare facilities. However, we recognize that such an implementation and
276 surveillance framework require a robust infrastructure, which may be challenging to establish in low-
277 and middle-income countries.

278 Overall, we described a six-plex dPCR assay targeting four respiratory viruses and its application to
279 Swiss wastewater. This allowed the identification and description of viral epidemiological trends at high
280 temporal resolution over one entire year. The results demonstrated that tracking of priority clinical
281 respiratory pathogens in wastewater provides data complementary to clinical-based surveillance. We
282 believe that continued surveillance is crucial for long-term analysis and will provide insights into
283 epidemiological trends and a more comprehensive understanding of pathogen dynamics over time,
284 enabling more effective public health interventions.

285 **MATERIALS AND METHODS**

286 **Experimental design**

287 We developed a six-plex digital PCR (dPCR) assay targeting four respiratory viruses: SARS-CoV-2 N1
288 and N2 genes (N1 and N2), Influenza A M gene (IAV-M), Influenza B M gene (IBV-M), and Respiratory
289 Syncytial Virus N gene (RSV-N), as well as Murine Hepatitis Virus M gene (MHV-M) which is used as
290 an internal control for RNA extraction efficiency. The assay was applied to wastewater samples collected
291 four or five times per week at 14 wastewater treatment plants from the 10th of July 2023 until the 22nd of
292 July 2024.

293 **Wastewater treatment plants**

294 Fourteen wastewater treatment plants (WWTPs) were monitored across Switzerland. The treatment
295 plants provide service to approximately 2.3 million inhabitants across different regions ([Supplemental
296 Table S1](#)), which corresponds to 26% of the national population.

297 **Wastewater sample processing and nucleic acid extraction**

298 Raw 24-hour composite wastewater samples, routinely collected by WWTP personnel, were stored at
299 4°C and transported on ice to our laboratory at the Swiss Federal Institute of Aquatic Science and
300 Technology (Eawag) in Dübendorf once a week. Samples were processed on the day of reception at
301 Eawag which resulted in a delay between collection and processing of 2-7 days depending on the
302 sample. Generally, five samples from each WWTP were processed weekly before 1st June 2024, then
303 four per week afterwards.

304 For each sample, nucleic acids were extracted from 40 mL of wastewater using a modified version of
305 the Wizard Enviro Total Nucleic Acid Kit (Promega Corporation, USA, Cat. No. A2991), as previously
306 described¹⁵. A blank extraction control, consisting of tap water, was included in each extraction run to
307 control for contamination during extraction. Nucleic acids were eluted in 80 µL RNase-free water and
308 then purified using the OneStep PCR Inhibitor Removal Kit (Zymo Research, USA, Cat. No. D6030).
309 Prior to dPCR analysis, extracts were further diluted in RNase-free water to minimize PCR inhibition
310 (generally three-fold, however five-fold for Chur, Lugano, Basel and Geneva from August 2023 to March
311 2024). Typically, extracts were analyzed using dPCR immediately following their preparation on the
312 same day. Extracts were stored for long-term preservation at -80°C.

313 **Positive controls**

314 Positive controls used in dPCR assays were prepared by combining and mixing nucleic acid templates
315 to achieve approximately 500 gene copies per µL for each target. Synthetic viral RNA was used for
316 SARS-CoV-2, whereas gBlocks® were used for Influenza A and B, and RSV. Positive material for MHV
317 was obtained by extracting RNA from cultured material ([Supplemental Table S6](#)).

318 **Digital PCR assays**

319 All dPCR assays were developed on the Naica® system 6-color Crystal Digital PCR Prism-6 (Stilla
320 Technologies, France). In this study, a six-plex assay, referred to as RESPV6, was developed. RESPV6
321 was created by merging two previous assays used in the Swiss monitoring program: i) a duplex assay
322 (targeting the SARS-CoV-2 nucleoprotein gene locus 1 [N1] and the MHV matrix protein [M]), and ii) a
323 previously described four-plex assay, known as RESPV4, with some modifications¹⁵. The RESPV4 was

324 adapted for targeting the SARS-CoV-2 nucleoprotein gene locus 2 (N2), the Influenza A and B matrix
325 protein genes (M), and the Respiratory Syncytial virus nucleoprotein gene (N). Primers and probes are
326 listed and described in **Table 1** and were purchased from Microsynth AG or IDT (Switzerland).

327 The RESPV6 assay was prepared using a total 27 μL pre-reaction volume, which consisted of 5.4 μL of
328 template and 21.6 μL of mastermix. The mastermix was prepared as follows: qScript XLT One-Step RT-
329 qPCR ToughMix (2x) (Quantabio, USA, Cat. No. 95132), 0.5 μM of each forward and reverse primer,
330 0.2 μM of each probe, SARS-N2 CDC Kit (0.125 μM of probe, 0.5 μM of primers, Integrated DNA
331 Technologies, USA, Cat. No. 10006713), 0.05 μM of fluorescein sodium salt (VWR, Cat. No. 0681-
332 100G), and RNase-free water. The reaction volume (25 μL) was loaded into Sapphire chips (Stilla
333 Technologies). Chips were loaded into a Geode (Stilla Technologies) which partitions the mastermix
334 into droplets (12 min at 40°C; droplet volume: 0.519 nL) before thermocycling using the following
335 conditions: reverse transcription (50°C for 1 h), enzyme activation (95°C for 5 min), and 40 cycles of
336 denaturation (95°C for 30 s) and annealing/extension (57.5°C for 1 min).

337 One Geode can run three Sapphire chips in parallel, each containing four chambers, such that 12
338 samples can be analyzed at once. Generally, five wastewater nucleic acid extracts were run in technical
339 duplicates, alongside a positive control and a no-template control (NTC). To pass quality control the
340 positive control must have signal and the NTC must have fewer than three positive partitions.
341 Additionally, there should be a minimum of 15'000 analyzable droplets. Reported data are the average
342 of the technical replicates, although chamber failure occasionally occurred resulting in data from a
343 singlet being taken. Reported data are the average of the technical replicates, although chamber failure
344 occasionally occurred resulting in data from a singlet being taken. Our dPCR setup follows the digital
345 MIQE (dMIQE) guidelines³⁴ as detailed in [Annex 1](#).

346 **PCR inhibition quality control**

347 PCR inhibition in the RESPV6 assay was evaluated using a three-step approach as previously
348 described²². First, the sample was analyzed to quantify the SARS-N1 target present in the wastewater
349 matrix using the RESPV6 assay. In the second step, a known quantity of SARS-N1 RNA was spiked
350 into the extract (approximately 750 gene copies per reaction), and the total SARS-N1 concentration was
351 measured again with the same RESPV6 assay. Finally, inhibition was calculated using the following
352 equation (1):

$$353 \quad \text{Inhibition (\%)} = 1 - \left(\frac{C_{\text{observed}}}{C_{\text{original}} + C_{\text{spike}}} \right) \quad (1)$$

354 where: C_{observed} is the concentration of SARS-N1 measured after spiking the sample with a known
355 quantity of SARS-N1, C_{original} is the concentration of SARS-N1 in the unspiked samples, and C_{spike} is the
356 concentration of SARS-N1 added as the spike-in.

357 An inhibition value of 0% indicated no inhibition, suggesting that the PCR reaction efficiency was
358 unaffected by the sample matrix. Conversely, a value of 100% indicated complete inhibition, where the
359 PCR amplification of the measured concentration in the spiked assay resulted in no detection of the N1
360 assay in the wastewater extract. Values between 0 and 100% reflected partial inhibition, with higher
361 values indicating higher levels of inhibition. Negative inhibition values, which are observed when C_{observed}

362 is higher than the sum of C_{original} and C_{spike} , are due to experimental variability, and are interpreted as an
363 absence of inhibition. Our internal threshold for re-running a sample was set at 40%; samples with
364 inhibition values above this threshold were considered inhibited and were subjected to re-analysis at a
365 higher dilution to reduce inhibition depending on concentrations of SARS-CoV-2 in the wastewater.
366 SARS-N1 inhibition served as a representative for the other targets. Measured RNA concentration was
367 not corrected based on the quantitative estimates of inhibition.

368 RNA extraction efficiency quality control

369 To determine the efficiency of RNA extraction, a known amount of viral control (Murine Hepatitis Virus
370 strain MHV-A59, or MHV) was spiked into wastewater prior to processing (target concentration: 10'000
371 gene copies per ml of wastewater⁸) and measured using dPCR in the resultant extract. Culturing of MHV
372 was performed in delayed brain tumor cells, at the École Polytechnique Fédérale de Lausanne (EPFL),
373 as previously described³⁵. Three out of every five samples (two out of every four samples after the 1st
374 June 2024) per week per WWTP were spiked with MHV. The recovery was determined by dividing the
375 measured concentration by the estimated spiked concentration and expressing the result as a
376 percentage. Measured RNA concentration was not corrected based on the quantitative estimates of the
377 extraction efficiency.

378 Data analysis and viral load calculation

379 All dPCR data were analyzed using the Crystal Miner Software version 4.0 (Stilla Technologies), which
380 provides RNA quantities expressed as gene copies per microliter of reaction (gc/ μ l of reaction).
381 Wastewater samples were defined as positive when the concentration was above the limit of detection
382 (LoD), which was set at approximately five gc per reaction, and corresponds to a threshold of at least
383 three positive partitions. Values were transformed to gene copies per liter of wastewater (gc/L_{ww}),
384 according to the following equation (2):

$$385 \quad \text{Conc.} \left(\frac{\text{gc}}{\text{L}_{\text{ww}}} \right) = \text{PCR conc.} \left(\frac{\text{gc}}{\mu\text{l}} \text{ rxn} \right) \times \text{dilution factor} \times \frac{\text{Reaction vol.}(\mu\text{l})}{\text{Template vol.}(\mu\text{l})} \times \frac{\text{Elution vol.}(\mu\text{l})}{\text{Wastewater vol.}(\text{ml})} \times 1000 \quad (2)$$

386 Viral RNA concentrations were adjusted by multiplying with the flow rate on the day of sampling at the
387 influent of the WWTP and dividing by population in the catchment area. These values are referred to as
388 viral loads and are expressed in gene copies per person per day (gc person⁻¹ day⁻¹).

389 A national median of viral loads was obtained by taking the median value over the WWTPs which have
390 data for a particular day. The centered seven-day rolling median of these data points was then taken to
391 visualize the trend.

392 Comparison with clinical data from different sources

393 The Swiss Federal Office of Public Health (FOPH) collects clinical data about respiratory viruses mainly
394 through two survey systems: the mandatory reporting system and the Swiss Sentinel System
395 (Sentinella)³⁶. The mandatory reporting system provides clinical data (i.e., clinical cases) for SARS-CoV-
396 2, Influenza A and Influenza B. Publicly available data from the mandatory reporting system are grouped
397 per week for the total Swiss population (8'855'062 inhabitants in 2024, including 39'677 inhabitants from
398 Liechtenstein), and additionally the SARS-CoV-2 data is stratified by geographical location at the
399 cantonal level. For this study, we additionally obtained data from the FOPH at daily resolution and
400 stratified by canton. In contrast, the Sentinella system is a voluntary reporting system involving around

401 160 to 180 medical doctors and provides data for the four pathogens covered by our RESPV6 assay,
402 including RSV³⁶. Sentinella data are only available as total number of cases reported per week with no
403 geographical location information available.

404 Since public case data for all the pathogens was only available at the national level, the national median
405 of viral loads in wastewater was used for comparison. Additionally, due to the clinical data being grouped
406 by week we computed a weekly average of our national wastewater load data by taking the mean daily
407 value for each of the targets for each week. These national weekly averages were used for correlation
408 analysis with case data.

409 Time-lagged cross-correlation analyses were performed to detect possible lag relationships between
410 the viral loads in wastewater and clinical cases for each of the four pathogens. Wastewater data was
411 shifted forward by a maximum of four weeks and cross-correlation was computed using Pearson
412 correlation. Correlation analysis and time-lagged cross-correlation were also carried out on the daily
413 resolution clinical data made available by the FOPH. Here, there was no requirement to aggregate
414 wastewater viral load data. Case data at the cantonal level was matched to wastewater load data based
415 on the canton where the WWTP is located ([Supplemental Table S1](#)).

416 **DATA AVAILABILITY**

417 Digital PCR data are available for download from wise.ethz.ch. Only data which passed our described
418 quality control processes are available here. All data is available on request. Weekly case data are
419 available from the Federal Office of Public Health (FOPH) via a public [API](#). Daily case data were
420 specifically requested from the FOPH. All code used in the analysis is available on [GitHub](#).

421 REFERENCES

- 422 1 Troeger, C. *et al.* Estimates of the global, regional, and national morbidity, mortality, and
423 aetiologies of lower respiratory tract infections in 195 countries: a systematic analysis for the
424 Global Burden of Disease Study 2015. *The Lancet Infectious Diseases* **17**, 1133-1161 (2017).
425 [https://doi.org/10.1016/S1473-3099\(17\)30396-1](https://doi.org/10.1016/S1473-3099(17)30396-1)
- 426 2 Hirve, S. *et al.* Influenza Seasonality in the Tropics and Subtropics - When to Vaccinate? *PLoS*
427 *One* **11**, e0153003 (2016). <https://doi.org/10.1371/journal.pone.0153003>
- 428 3 Reed, C. *et al.* Estimating influenza disease burden from population-based surveillance data in
429 the United States. *PLoS One* **10**, e0118369 (2015).
430 <https://doi.org/10.1371/journal.pone.0118369>
- 431 4 Xagorarakis, I. & O'Brien, E. in *Women in Water Quality: Investigations by Prominent Female*
432 *Engineers* (ed Deborah Jean O'Bannon) 75-97 (Springer International Publishing, 2020).
- 433 5 Sims, N. & Kasprzyk-Hordern, B. Future perspectives of wastewater-based epidemiology:
434 Monitoring infectious disease spread and resistance to the community level. *Environment*
435 *International* **139**, 105689 (2020).
436 <https://doi.org/10.1016/j.envint.2020.105689>
- 437 6 Medema, G., Heijnen, L., Elsinga, G., Italiaander, R. & Brouwer, A. Presence of SARS-
438 Coronavirus-2 RNA in Sewage and Correlation with Reported COVID-19 Prevalence in the Early
439 Stage of the Epidemic in The Netherlands. *Environmental Science & Technology Letters* **7**, 511-
440 516 (2020). <https://doi.org/10.1021/acs.estlett.0c00357>
- 441 7 Medema, G., Been, F., Heijnen, L. & Petterson, S. Implementation of environmental
442 surveillance for SARS-CoV-2 virus to support public health decisions: Opportunities and
443 challenges. *Current Opinion in Environmental Science & Health* **17**, 49-71 (2020).
444 <https://doi.org/10.1016/j.coesh.2020.09.006>
- 445 8 Fernandez-Cassi, X. *et al.* Wastewater monitoring outperforms case numbers as a tool to track
446 COVID-19 incidence dynamics when test positivity rates are high. *Water Res* **200**, 117252
447 (2021). <https://doi.org/10.1016/j.watres.2021.117252>
- 448 9 Peccia, J. *et al.* Measurement of SARS-CoV-2 RNA in wastewater tracks community infection
449 dynamics. *Nature Biotechnology* **38**, 1164-1167 (2020). [https://doi.org/10.1038/s41587-020-](https://doi.org/10.1038/s41587-020-0684-z)
450 [0684-z](https://doi.org/10.1038/s41587-020-0684-z)
- 451 10 Kilaru, P. *et al.* Wastewater Surveillance for Infectious Disease: A Systematic Review. *American*
452 *Journal of Epidemiology* **192**, 305-322 (2022). <https://doi.org/10.1093/aje/kwac175>
- 453 11 Hughes, B. *et al.* Respiratory Syncytial Virus (RSV) RNA in Wastewater Settled Solids Reflects
454 RSV Clinical Positivity Rates. *Environmental Science & Technology Letters* **9**, 173-178 (2022).
455 <https://doi.org/10.1021/acs.estlett.1c00963>
- 456 12 Wolfe, M. K. *et al.* Wastewater-Based Detection of Two Influenza Outbreaks. *Environmental*
457 *Science & Technology Letters* **9**, 687-692 (2022). <https://doi.org/10.1021/acs.estlett.2c00350>
- 458 13 Zheng, X. *et al.* Development and application of influenza virus wastewater surveillance in
459 Hong Kong. *Water Research* **245**, 120594 (2023).
460 <https://doi.org/10.1016/j.watres.2023.120594>
- 461 14 Whale, A. S., Huggett, J. F. & Tzonev, S. Fundamentals of multiplexing with digital PCR.
462 *Biomolecular Detection and Quantification* **10**, 15-23 (2016).
463 <https://doi.org/10.1016/j.bdq.2016.05.002>
- 464 15 Nadeau, S. *et al.* Influenza transmission dynamics quantified from RNA in wastewater in
465 Switzerland. *Swiss Medical Weekly* **154**, 3503 (2024). <https://doi.org/10.57187/s.3503>

- 466 16 *WISE Dashboard - Wastewater-based Infectious Disease Surveillance and Epidemiology*,
467 <<https://wise.ethz.ch/>> (Accessed on: 01/11/2024).
- 468 17 Zheng, X. *et al.* Comparison of virus concentration methods and RNA extraction methods for
469 SARS-CoV-2 wastewater surveillance. *Science of The Total Environment* **824**, 153687 (2022).
470 <https://doi.org/https://doi.org/10.1016/j.scitotenv.2022.153687>
- 471 18 Ahmed, W. *et al.* Comparison of virus concentration methods for the RT-qPCR-based recovery
472 of murine hepatitis virus, a surrogate for SARS-CoV-2 from untreated wastewater. *Science of*
473 *The Total Environment* **739**, 139960 (2020).
474 <https://doi.org/https://doi.org/10.1016/j.scitotenv.2020.139960>
- 475 19 Hart, J. J., Jamison, M. N., McNair, J. N. & Szlag, D. C. Frequency and degradation of SARS-CoV-
476 2 markers N1, N2, and E in sewage. *Journal of Water and Health* **21**, 514-524 (2023).
477 <https://doi.org/10.2166/wh.2023.314>
- 478 20 Sun, J. *et al.* Underestimation of SARS-CoV-2 in wastewater due to single or double mutations
479 in the N1 qPCR probe binding region. *Water Research X* **22**, 100221 (2024).
480 <https://doi.org/https://doi.org/10.1016/j.wroa.2024.100221>
- 481 21 Chen, C. *et al.* CoV-Spectrum: analysis of globally shared SARS-CoV-2 data to identify and
482 characterize new variants. *Bioinformatics* **38**, 1735-1737 (2021).
483 <https://doi.org/10.1093/bioinformatics/btab856>
- 484 22 Huisman Jana, S. *et al.* Wastewater-Based Estimation of the Effective Reproductive Number of
485 SARS-CoV-2. *Environmental Health Perspectives* **130**, 057011
486 <https://doi.org/10.1289/EHP10050>
- 487 23 *Similarities and Differences between Flu and COVID-19*,
488 <<https://www.cdc.gov/flu/symptoms/flu-vs-covid19.htm>> (Accessed on: 16/05/2024).
- 489 24 Aliza Rosen, M. H. *What to Know About JN.1, the Latest Omicron Variant*,
490 <<https://publichealth.jhu.edu/2024/jn1-the-dominant-variant-in-the-covid-surge>> (2024)
491 Accessed on: 15/05/2024).
- 492 25 Idris, I. & Adesola, R. O. Emergence and spread of JN.1 COVID-19 variant. *Bulletin of the*
493 *National Research Centre* **48**, 27 (2024). <https://doi.org/10.1186/s42269-024-01183-5>
- 494 26 Kaku, Y. *et al.* Virological characteristics of the SARS-CoV-2 KP.2 variant. *bioRxiv*,
495 2024.2004.2024.590786 (2024). <https://doi.org/10.1101/2024.04.24.590786>
- 496 27 Faherty, E. A. G. *et al.* Correlation of wastewater surveillance data with traditional influenza
497 surveillance measures in Cook County, Illinois, October 2022–April 2023. *Science of The Total*
498 *Environment* **912**, 169551 (2024).
499 <https://doi.org/https://doi.org/10.1016/j.scitotenv.2023.169551>
- 500 28 Wolken, M. *et al.* Wastewater surveillance of SARS-CoV-2 and influenza in preK-12 schools
501 shows school, community, and citywide infections. *Water Research* **231**, 119648 (2023).
502 <https://doi.org/https://doi.org/10.1016/j.watres.2023.119648>
- 503 29 Wade, M. J. *et al.* Understanding and managing uncertainty and variability for wastewater
504 monitoring beyond the pandemic: Lessons learned from the United Kingdom national COVID-
505 19 surveillance programmes. *Journal of Hazardous Materials* **424**, 127456 (2022).
506 <https://doi.org/https://doi.org/10.1016/j.jhazmat.2021.127456>
- 507 30 Ahmed, W. *et al.* SARS-CoV-2 RNA monitoring in wastewater as a potential early warning
508 system for COVID-19 transmission in the community: A temporal case study. *Science of The*
509 *Total Environment* **761**, 144216 (2021).
510 <https://doi.org/https://doi.org/10.1016/j.scitotenv.2020.144216>

- 511 31 Wu, F. *et al.* SARS-CoV-2 RNA concentrations in wastewater foreshadow dynamics and clinical
512 presentation of new COVID-19 cases. *Science of The Total Environment* **805**, 150121 (2022).
513 <https://doi.org/https://doi.org/10.1016/j.scitotenv.2021.150121>
- 514 32 Weidhaas, J. *et al.* Correlation of SARS-CoV-2 RNA in wastewater with COVID-19 disease
515 burden in sewersheds. *Science of The Total Environment* **775**, 145790 (2021).
516 <https://doi.org/https://doi.org/10.1016/j.scitotenv.2021.145790>
- 517 33 Rezaeitavabe, F. *et al.* Beyond linear regression: Modeling COVID-19 clinical cases with
518 wastewater surveillance of SARS-CoV-2 for the city of Athens and Ohio University campus.
519 *Science of The Total Environment* **912**, 169028 (2024).
520 <https://doi.org/https://doi.org/10.1016/j.scitotenv.2023.169028>
- 521 34 Group, T. d. & Huggett, J. F. The Digital MIQE Guidelines Update: Minimum Information for
522 Publication of Quantitative Digital PCR Experiments for 2020. *Clinical Chemistry* **66**, 1012-1029
523 (2020). <https://doi.org/10.1093/clinchem/hvaa125>
- 524 35 Leibowitz, J., Kaufman, G. & Liu, P. Coronaviruses: propagation, quantification, storage, and
525 construction of recombinant mouse hepatitis virus. *Curr Protoc Microbiol* **Chapter 15**, Unit 15E
526 11 (2011). <https://doi.org/10.1002/9780471729259.mc15e01s21>
- 527 36 <<https://idd.bag.admin.ch/survey-systems/oblig>> (Accessed on: 15/4/2024).
- 528 37 Ward, C. L. *et al.* Design and performance testing of quantitative real time PCR assays for
529 influenza A and B viral load measurement. *Journal of Clinical Virology* **29**, 179-188 (2004).
530 [https://doi.org/https://doi.org/10.1016/S1386-6532\(03\)00122-7](https://doi.org/https://doi.org/10.1016/S1386-6532(03)00122-7)
- 531 38 Lu, X. *et al.* US CDC Real-Time Reverse Transcription PCR Panel for Detection of Severe Acute
532 Respiratory Syndrome Coronavirus 2. *Emerg Infect Dis* **26**, 1654-1665 (2020).
533 <https://doi.org/10.3201/eid2608.201246>
- 534

535 **ACKNOWLEDGEMENTS**

536 We would like to thank present and past members of the Laboratory Monitoring Team for developing
537 the methods, processing samples and generating and analyzing data. Additionally, we thank present
538 and past collaborators of the WISE (Wastewater-based Infectious disease Surveillance and
539 Epidemiology) project for their support and valuable intellectual contributions, and NEXUS for their
540 setting up and supporting the WISE database (wisedb.ethz.ch) which facilitated our analysis. We thank
541 the technical staff of each WWTP for promptly sending us the wastewater samples on a weekly basis,
542 and Anna Carratala Ripolles and Tamar Kohn for providing us with MHV.

543 **AUTHORS' CONTRIBUTIONS**

544 CO and TRJ conceptualized, supervised, and provided funding. MP and REM designed the study,
545 performed analyses, prepared visualizations, and wrote the first draft of the manuscript. LC, JdK, CG,
546 and SK contributed invaluable scientific insights. PS provided statistical support. AD, CH, AH, GL, LS,
547 AW, and DY helped with sample processing, data generation and curation. All authors reviewed, edited,
548 and approved the final version.

549 **FUNDING**

550 This study was funded by the Swiss National Science Foundation (SNSF Sinergia Grant Nr.
551 CRSII5_205933) and by the Swiss Federal Office of Public Health grant to CO and TRJ.

552 **CONFLICTS OF INTEREST**

553 None.

554 **AUTHORS' STATEMENT**

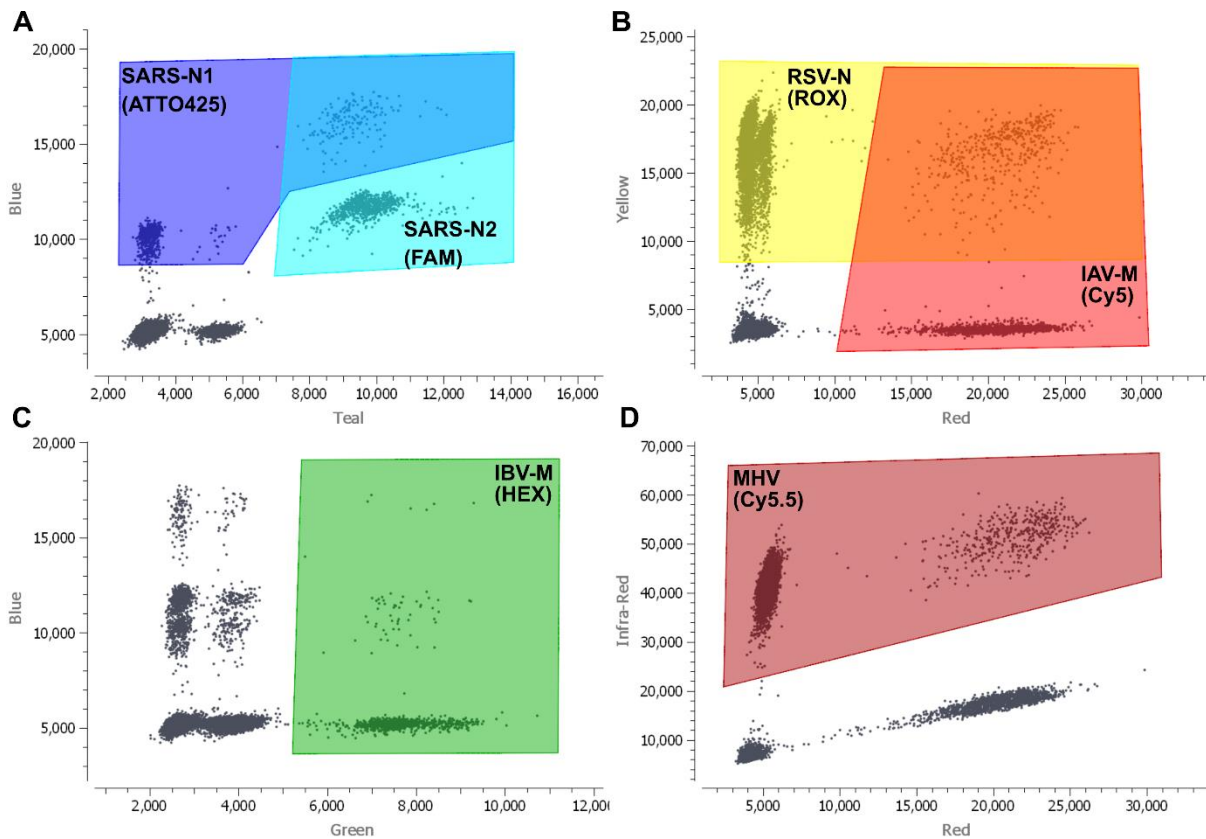
555 We declare that all authors have seen and approved the manuscript and have contributed significantly
556 to the work. Some data and figures from the manuscript presented here have been used to create a
557 report to the primary funding body, the Swiss Federal Office of Public Health. The report was briefly
558 made public (September – November 2024).

559 **TABLES**560 **Table 1. Primers and probes of the RESPV6 dPCR assay used in this study.**

Oligonucleotide name	Sequence (5' to 3')	Fluorophore / Quencher	Pathogen	Gene	Type	Reference
RSV-6p-F	CTC CAG AAT AYA GGC ATG AYT CTC C		Respiratory Syncytial Virus	N	Forward primer	Hughes, et al. ¹¹
RSV-6p-R	GCY CTY CTA ATY ACW GCT GTA AGA C		Respiratory Syncytial Virus	N	Reverse primer	Hughes, et al. ¹¹
RSV-6p-P	TAA CCA AAT TAG CAG CAG GAG ATA GAT CAG	ROX/BHQ-2	Respiratory Syncytial Virus	N	Probe	Hughes, et al. ¹¹
IAV-6p-F	TGG AAT GGC TAA AGA CAA GAC CAA T		Influenza A Virus	M	Forward primer	Modified from Ward, et al. ³⁷
IAV-6p-R	AAA GCG TCT ACG CTG CAG TCC		Influenza A Virus	M	Reverse primer	Modified from Ward, et al. ³⁷
IAV-6p-P	TTT GTK TTC ACG CTC ACC GTG CCC	Cy5/BHQ-2	Influenza A Virus	M	Probe	Modified from Ward, et al. ³⁷
IBV-6p-F	GAG ACA CAA TTG CCT ACY TGC TT		Influenza B Virus	M	Forward primer	Modified from Ward, et al. ³⁷
IBV-6p-R	ATT CTT TCC CAC CRA ACC AAC A		Influenza B Virus	M	Reverse primer	Modified from Ward, et al. ³⁷
IBV-6p-P	AGA AGA TGG AGA AGG CAA AGC AGA ACT AGC	HEX/BHQ-1	Influenza B Virus	M	Probe	Modified from Ward, et al. ³⁷
SARSN1-6p-F	GAC CCC AAA ATC AGC GAA AT		SARS-CoV-2	N1	Forward primer	Lu, et al. ³⁸
SARSN1-6p-R	TCT GGT TAC TGC CAG TTG AAT CTG		SARS-CoV-2	N1	Reverse primer	Lu, et al. ³⁸
SARSN1-6p-P	ACC CCG CAT TAC GTT TGG TGG ACC	ATTO425/BHQ-1	SARS-CoV-2	N1	Probe	Lu, et al. ³⁸
MHV-6p-F	GGA ACT TCT CGT TGG GCA TTA TAC T		Murine Hepatitis Virus		Forward primer	Ahmed, et al. ¹⁸
MHV-6p-R	ACC ACA AGA TTA TCA TTT TCA CAA CAT A		Murine Hepatitis Virus		Reverse primer	Ahmed, et al. ¹⁸
MHV-6p-P	ACA TGC TAC GGC TCG TGT AAC CGA ACT GT	Cy5.5/BHQ-3	Murine Hepatitis Virus		Probe	Ahmed, et al. ¹⁸
SARS-N2 CDC Kit		FAM	SARS-CoV-2	N2	Kit	2019-nCoV RUO Kit (Integrated DNA Technologies)

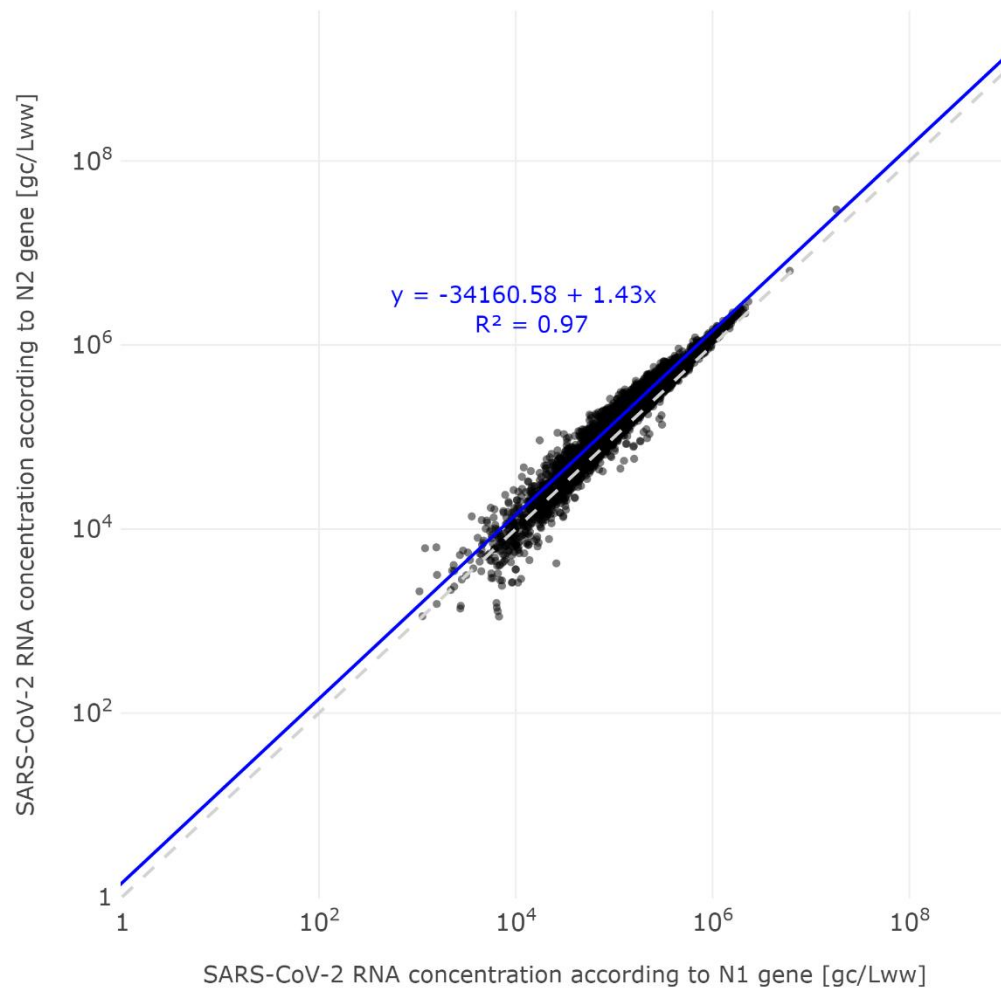
561

562 **FIGURES**



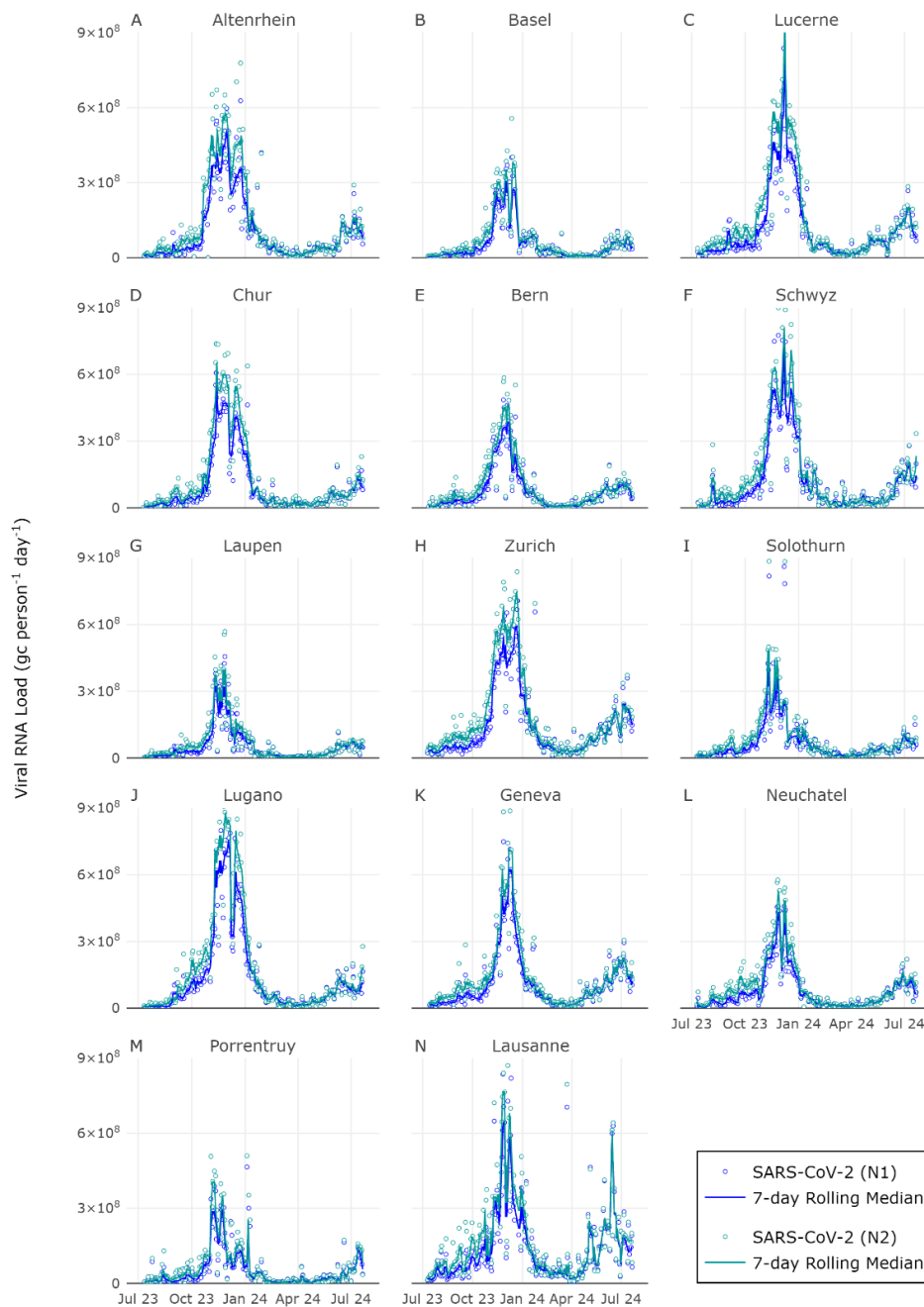
563

564 **Figure 1. Two-dimensional visualization of the partition classification of RESPV6 dPCR assay**
565 **after measuring positive control.** Both x-axes and y-axes show fluorescence intensities. Titles on
566 axes indicate the fluorescent channel. Each black dot corresponds to a dPCR partition. Partitions are
567 classified by manually drawing polygons. Investigated targets are shown in bold within polygons with
568 fluorophores in parentheses. Partitions enclosed in the area where polygons overlap are positive for
569 multiple targets (i.e., one partition contains two or more targets). **(A)** SARS-CoV-2 genes N1 and N2
570 can both be gated in teal and blue channels. **(B)** RSV-N and IAV-M can be gated in yellow and red
571 channels, respectively. **(C)** IBV-M positive clusters are separable in the green channel. **(D)** MHV is gated
572 in the infra-red channel. This figure has been formatted using Inkscape.



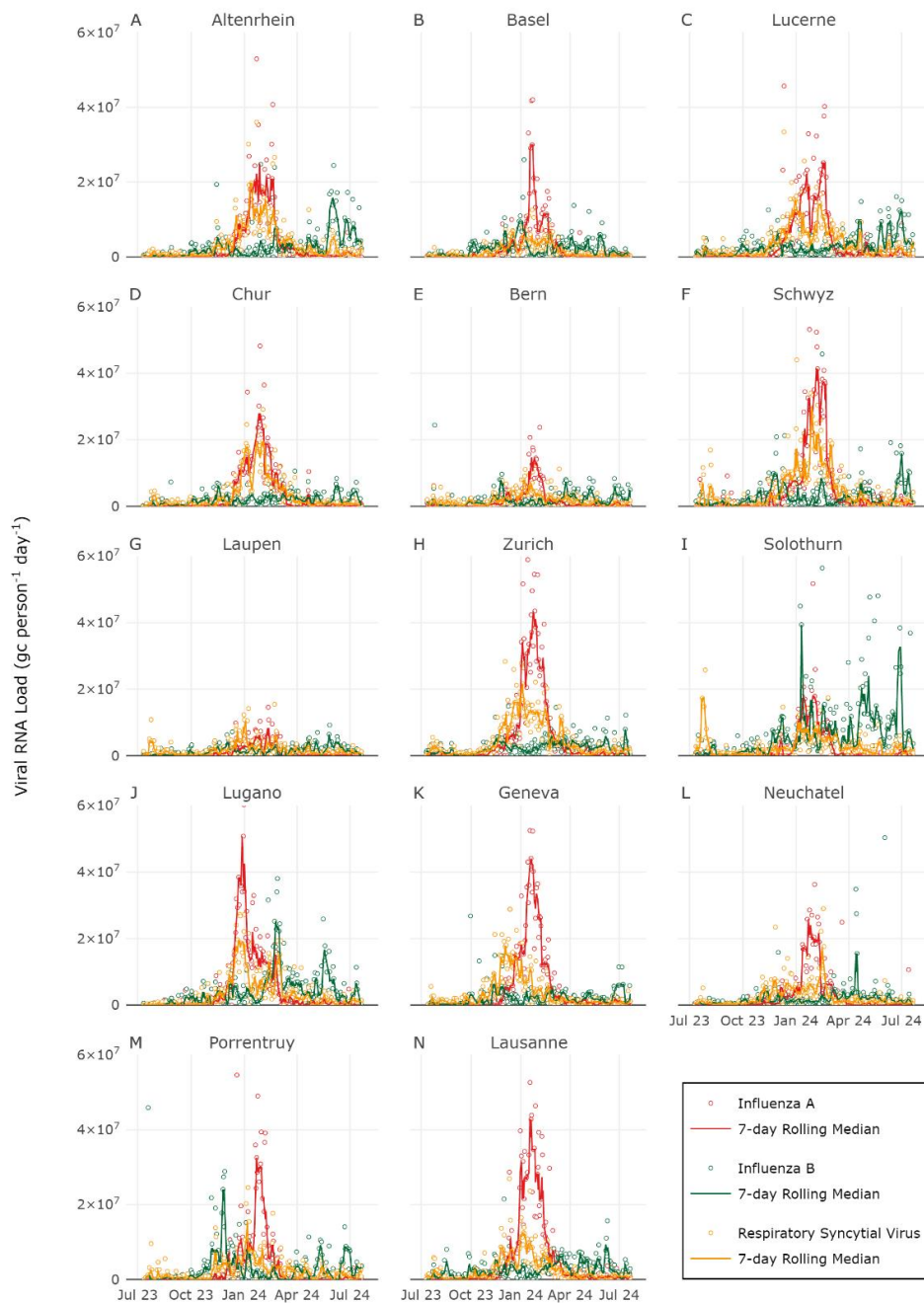
573

574 **Figure 2. SARS-CoV-2 RNA concentrations comparing N1 and N2 genes.** Concentrations are
575 expressed in gene copies per liter of wastewater (gc/Lww) and shown on a log scale. The grey dashed
576 line indicates the identity line. The linear regression line is shown in blue.



577

578 **Figure 3. SARS-CoV-2 N1 and N2 load in wastewater across 14 Swiss locations.** SARS-CoV-2
579 RNA loads, expressed in gene copies (gc) per person per day, were calculated for N1 and N2 genes.
580 Measured RNA loads are represented with a circle (blue for SARS-N1 and teal for SARS-N2), whereas
581 the respective seven-day rolling medians are displayed with solid lines. Each panel indicates a different
582 WWTP. For visualization purposes, some very high load values are not visible in the plots and are listed
583 in [Supplemental Table S7](#).



584

585 **Figure 4. Influenza A, Influenza B and RSV RNA loads in wastewater across 14 Swiss locations.**

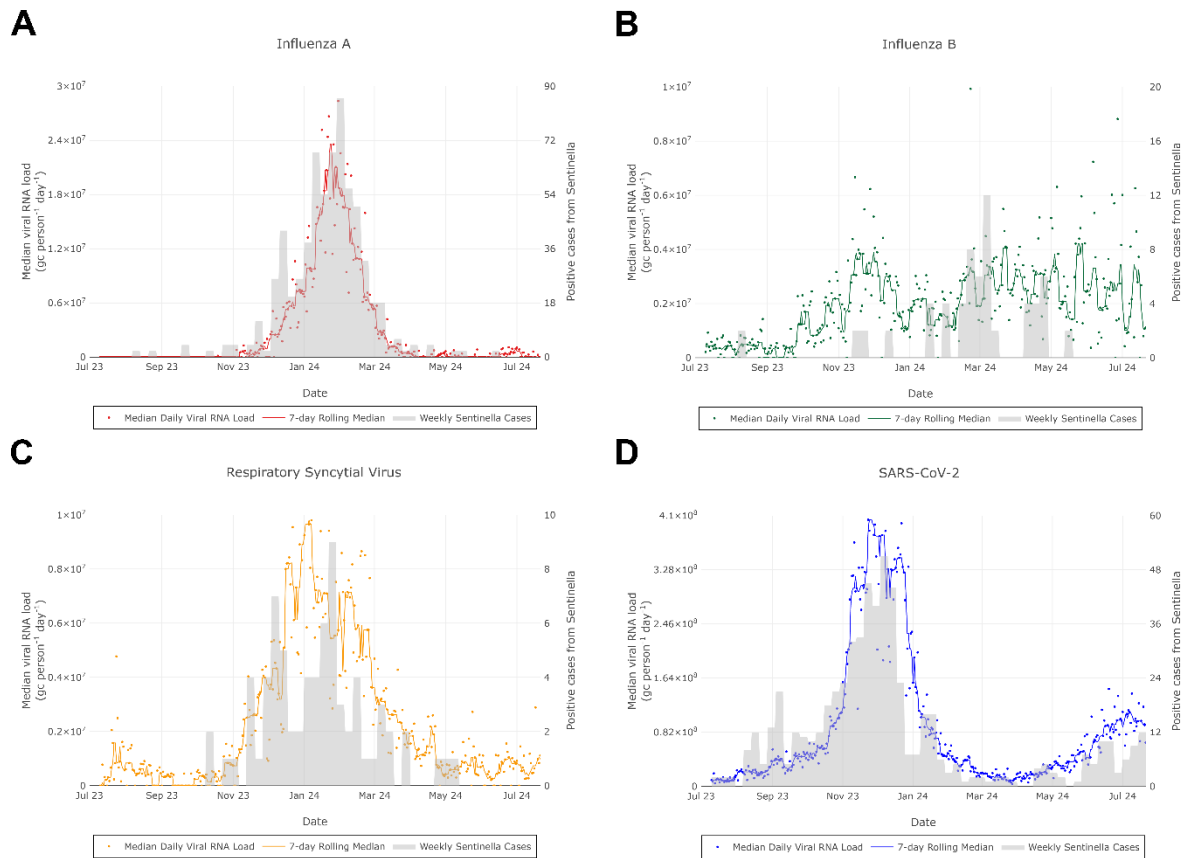
586 Viral RNA loads were expressed in gene copies (gc) per person per day. Measured RNA loads are

587 represented with a circle (red for IAV, green for IBV, and yellow for RSV), whereas the respective seven-

588 day rolling median is displayed with solid lines. Each panel indicates a different WWTP. For visualization

589 purposes, some very high load values are not visible in the plots and are listed in [Supplemental Table](#)

590 [S7](#).



591

592 **Figure 5. Comparison of viral RNA loads in wastewater and number of cases from Sentinella**
593 **system.** Positive cases, expressed in absolute numbers, refer to the entire Swiss territory, and were
594 taken from the Sentinella database. Cases are shown using light grey bars. Some high load values are
595 beyond the plotted y-max values. They are listed in [Supplemental Table S7](#). This figure has been
596 formatted using Inkscape.